Available online at www.sciencedirect.com
ScienceDirect
Journal of Sound and Vibration 310 (2008) 702–717
JOURNAL OF SOUND AND VIBRATION
www.elsevier.com/locate/jsvi

Transition radiation of elastic waves at the interface of two elastic half-planes

Karel N. van Dalen*, Andrei V. Metrikine

Faculty of Civil Engineering and Geosciences, Delft University of Technology, P.O. Box 5048, 2600 GA Delft, The Netherlands

Accepted 11 June 2007
The peer review of this article was organised by the Guest Editor
Available online 7 August 2007

Abstract

Radiation of elastic waves is studied that is emitted by a point load that crosses the interface of two elastic half-planes. It is assumed that the load has a constant magnitude, moves along a straight line normal to the interface, and has a constant speed that is smaller than the minimum shear wave speed in the half-planes. In this case the mechanism of excitation of elastic waves is conventionally referred to as transition radiation. The adopted model allows to obtain an analytical expression for the elastic field excited by the load in the frequency–wavenumber domain. Using this expression, the energy of transition radiation is derived in a closed form. It is shown that transition radiation of the body waves occurs at any non-zero velocity of the load. Additionally, transition radiation of interface waves may occur provided that parameters of the half-planes allow existence of Stoneley waves. A parametric analysis of the directivity diagram of radiated body waves is accomplished focusing on dependence of the diagram on the load speed, load direction, and parameters of the half-planes. Using parameters that allow radiation of interface waves, the energy of this radiation is compared to that of the body waves. It is shown that the energy of the interface waves is greater unless the load velocity is close to the lowest body wave velocity.

1. Introduction

Transition radiation is emitted when a perturbation source (electric charge, acoustic monopole, mechanical load, etc.), that does not possess an inherent frequency, moves along a straight line at a constant velocity in an inhomogeneous medium or near such a medium [1]. For the first time, this phenomenon was described by Ginzburg and Frank [2] who analyzed radiation of electromagnetic waves by a charged particle crossing the boundary between an ideal conductor and vacuum. Already in early studies concerned with transition radiation, it was demonstrated that this phenomenon was universal from the physical point of view because it occurred irrespective of the physical nature of the waves. This provided a basis for the investigation into acoustic transition radiation initiated in 1962 which was then carried out in parallel with extensive studies on electromagnetic transition radiation [3]. Today, there are a vast number of reports on both the electromagnetic and acoustic radiation, and a monograph [1] which provides a comprehensive account of transition radiation in classical electrodynamics.

*Corresponding author. Faculty of Civil Engineering and Geosciences, Delft University of Technology, Stevinweg 1, 2628 CN Delft, The Netherlands. Tel.: +31 15 2788388; fax: +31 15 2781189.
E-mail address: k.n.vandalen@tudelft.nl (K.N. van Dalen).

0022-460X/$ - see front matter © 2007 Elsevier Ltd. All rights reserved.
doi:10.1016/j.jsv.2007.06.007

In the beginning of 1990s, the first study was published on transition radiation of elastic waves [4]. This radiation is emitted, for example, by every train running on a conventional railway track. The wheels of the train, pressed against the rails by gravity, excite elastic waves in the railway track due to track inhomogeneity caused by sleepers, non-uniform subsoil, etc. A review of the studies on transition radiation of elastic waves in one- and two-dimensional elastic systems (strings, beams, membranes and plates) can be found in Ref. [5].

This paper presents the first study of transition radiation of elastic waves in an elastic continuum. Such study is necessary to pave the way to physical understanding of ground vibration induced by high speed trains and associated with non-uniformity of the subsoil. For example the fundamentals of transition radiation have to be known to understand ground vibration generated by a train as it enters/leaves a bridge or passes by a railway station. Another example in which transition radiation plays the governing role is generation of ground vibration by underground trains that can be caused by variation of soil parameters along a train tunnel.

The aim of this paper is to discover the fundamental features of transition radiation in elastic continua and to compare these features to those known in electrodynamics, acoustics and structural mechanics (see Refs. [1–5]). To reach this aim, a basic model is chosen that consists of two elastic half-planes. The half-planes are subjected to a constant load that crosses the interface between the half-planes along the path normal to this interface. Though the chosen model has no direct practical application, its major advantage is that it allows to obtain an analytical expression for the energy of transition radiation.

This paper is structured as follows. In Section 2, the model is described and an expression is obtained for the elastic field that is excited by the load. In Section 3, the angular density of the energy of transition radiation is derived that is transferred by the body waves. In Section 4, it is shown that transition radiation of interface waves can also occur and a closed-form expression is found for the energy of this radiation. Finally, in Section 5, a parametric analysis of transition radiation is accomplished focusing on dependence of radiation on the load velocity and parameters of the half-planes.

2. Model, solution and radiation field

To study the fundamental features of transition radiation in elastic continua, a moving load is considered that crosses a sharp interface of two homogeneous isotropic elastic half-planes, as shown in Fig. 1. To ensure that transition radiation occurs in its pure form, the other possible radiation mechanisms should be prevented, namely the radiation due to a transient loading, the radiation due to a non-uniform motion and the Mach radiation. This is done by assuming that the load has a constant magnitude F_z and moves along a straight line $z = 0$ at a constant speed V, which is smaller than the minimum shear wave speed in the elastic continuum.

The load-induced motion of the elastic continuum, assuming the plane-strain and disregarding the transient effects associated with the start of the load, is described by the following equation of motion and interface conditions at $z = 0$:

$$c_{\mathrm{p}i}^2 \nabla(\nabla \cdot \mathbf{u}_i) - c_{\mathrm{s}i}^2 \nabla \times (\nabla \times \mathbf{u}_i) = \partial_{tt}\mathbf{u} - \mathbf{F}/\rho_i \delta(x - Vt)\delta(z), \tag{1}$$

$$\mathbf{u}_1 = \mathbf{u}_2, \quad \mathbf{t}_1^{(\mathbf{e}_x)} = \mathbf{t}_2^{(\mathbf{e}_x)}, \quad x = 0. \tag{2}$$

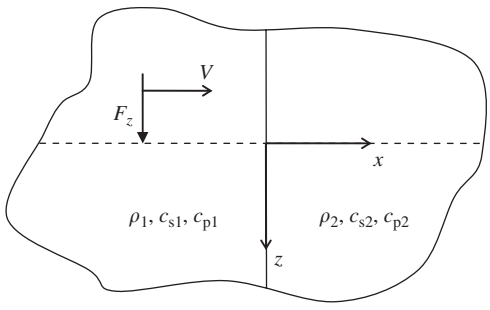

Fig. 1. Two homogeneous isotropic half-planes subjected to a uniformly moving load.

In Eq. (1), index i specifies the quantities belonging to the left ($i=1$) and the right ($i=2$) half-planes, $\mathbf{u}_i=[u_i(x,z,t)\ w_i(x,z,t)]^{\mathrm{T}}$ is the vector-displacement of the continuum, $c_{\mathrm{p}i}$ and $c_{\mathrm{s}i}$ are the pressure wave speed and the shear wave speed, ρ_i is the material density, $\mathbf{F}=[0\quad F_z]^{\mathrm{T}}$ is the load, V is the load speed, $\mathbf{t}_i^{(\mathbf{e}_x)}$ is the traction on a plane with the normal direction $\mathbf{e}_x$, $\nabla=\begin{bmatrix}\partial_x & \partial_z\end{bmatrix}^{\mathrm{T}}$, $\delta(\ldots)$ is the Dirac delta-function.

To analyze the problem, the following integral Fourier transform is applied to Eq. (1):

$$\tilde{\tilde{\mathbf{u}}}_i(x,\omega,k_z)=\int_{-\infty}^{\infty}\int_{-\infty}^{\infty}\mathbf{u}_i(x,z,t)\exp\left(\mathrm{i}(\omega t-k_z z)\right)\mathrm{d}t\,\mathrm{d}z, \tag{3}$$

where ω and k_z are the frequency and z-component of the wavenumber. This results in the following system of ordinary differential equations:

$$\begin{bmatrix}b_i^2 & 0\\ 0 & 1\end{bmatrix}\begin{bmatrix}\partial_{xx}\tilde{\tilde{u}}_i\\ \partial_{xx}\tilde{\tilde{w}}_i\end{bmatrix}+\mathrm{i}\left(b_i^2-1\right)k_z\begin{bmatrix}0 & 1\\ 1 & 0\end{bmatrix}\begin{bmatrix}\partial_x\tilde{\tilde{u}}_i\\ \partial_x\tilde{\tilde{w}}_i\end{bmatrix}+\begin{bmatrix}R_{\mathrm{s}i}^2 & 0\\ 0 & b_i^2R_{\mathrm{p}i}^2\end{bmatrix}\begin{bmatrix}\tilde{\tilde{u}}_i\\ \tilde{\tilde{w}}_i\end{bmatrix}=-\frac{1}{\mu_i V}\begin{bmatrix}0\\ F_z\end{bmatrix}\mathrm{e}^{\mathrm{i}\omega x/V}, \tag{4}$$

where $b_i=c_{\mathrm{p}i}/c_{\mathrm{s}i}<1$, $R_{\mathrm{s}i}^2=\omega^2/c_{\mathrm{s}i}^2-k_z^2$, $R_{\mathrm{p}i}^2=\omega^2/c_{\mathrm{p}i}^2-k_z^2$, and μ_i is the shear modulus.

Accounting for the proper behavior at $x\to\pm\infty$, the general solution of Eq. (4) can be written as

$$\tilde{\tilde{\mathbf{u}}}_i=\mathbf{A}_i\exp\left(\mathrm{i}\omega x/V\right)+d_{\mathrm{s}i}\mathbf{C}_{\mathrm{s}i}\exp\left(-\mathrm{i}R_{\mathrm{s}i}|x|\right)+d_{\mathrm{p}i}\mathbf{C}_{\mathrm{p}i}\exp\left(-\mathrm{i}R_{\mathrm{p}i}|x|\right), \tag{5}$$

where

$$\begin{aligned}&\mathbf{C}_{\mathrm{s}1}=\begin{bmatrix}1 & R_{\mathrm{s}1}/k_z\end{bmatrix}^{\mathrm{T}},\quad \mathbf{C}_{\mathrm{p}1}=\begin{bmatrix}1 & -k_z/R_{\mathrm{p}1}\end{bmatrix}^{\mathrm{T}},\quad \mathbf{C}_{\mathrm{s}2}=\begin{bmatrix}1 & -R_{\mathrm{s}2}/k_z\end{bmatrix}^{\mathrm{T}},\quad \mathbf{C}_{\mathrm{p}2}=\begin{bmatrix}1 & k_z/R_{\mathrm{p}2}\end{bmatrix}^{\mathrm{T}},\\ &\mathbf{A}_i=\begin{bmatrix}A_i & B_i\end{bmatrix}^{\mathrm{T}},\\ &A_i=-\frac{F_z\omega k_z\left(1-1/b_i^2\right)}{\mu_i V^2\left(R_{\mathrm{s}i}^2-\omega^2/V^2\right)\left(R_{\mathrm{p}i}^2-\omega^2/V^2\right)},\quad B_i=-\frac{F_z\left(R_{\mathrm{p}i}^2-\omega^2/V^2+\left(1-1/b_i^2\right)k_z^2\right)}{\mu_i V^2\left(R_{\mathrm{s}i}^2-\omega^2/V^2\right)\left(R_{\mathrm{p}i}^2-\omega^2/V^2\right)}\end{aligned} \tag{6}$$

and the radicals $R_{\mathrm{s}i}$ and $R_{\mathrm{p}i}$ are defined as

$$R_{\mathrm{s}i,\mathrm{p}i}=\sqrt{\omega^2/c_{\mathrm{s}i,\mathrm{p}i}^2-k_z^2}=\begin{cases}-\sqrt{\omega^2/c_{\mathrm{s}i,\mathrm{p}i}^2-k_z^2}, & \omega<-c_{\mathrm{s}i,\mathrm{p}i}|k_z|,\\ \mathrm{i}\sqrt{k_z^2-\omega^2/c_{\mathrm{s}i,\mathrm{p}i}^2}, & \omega^2\leqslant c_{\mathrm{s}i,\mathrm{p}i}^2k_z^2,\\ +\sqrt{\omega^2/c_{\mathrm{s}i,\mathrm{p}i}^2-k_z^2}, & \omega>+c_{\mathrm{s}i,\mathrm{p}i}|k_z|.\end{cases} \tag{7}$$

The above definition of the radicals satisfies the requirement of vanishing displacements at $x\to\pm\infty$ (for $\omega^2\leqslant c_{\mathrm{s}i,\mathrm{p}i}^2k_z^2$) and the radiation condition (for $\omega^2>c_{\mathrm{s}i,\mathrm{p}i}^2k_z^2$) which requires that no wave can propagate from infinity towards the interface of the half-planes.

To find the unknown amplitudes $d_{\mathrm{s}i}$ and $d_{\mathrm{p}i}$ in Eq. (5), the continuity of tractions and displacements at $z=0$ (Eq. (2)), has to be employed. Substitution of Eq. (5) into Eq. (2) gives a system of four linear algebraic equations, which can be written as

$$\begin{bmatrix}-1 & -1 & 1 & 1\\ -R_{\mathrm{s}1}/k_z & k_z/R_{\mathrm{p}1} & -R_{\mathrm{s}2}/k_z & k_z/R_{\mathrm{p}2}\\ 2R_{\mathrm{s}1} & \left(R_{\mathrm{s}1}^2-k_z^2\right)/R_{\mathrm{p}1} & 2\mu R_{\mathrm{s}2} & \mu\left(R_{\mathrm{s}2}^2-k_z^2\right)/R_{\mathrm{p}2}\\ \left(R_{\mathrm{s}1}^2-k_z^2\right)/k_z & -2k_z & -\mu\left(R_{\mathrm{s}2}^2-k_z^2\right)/k_z & 2\mu k_z\end{bmatrix}\begin{bmatrix}d_{\mathrm{s}1}\\ d_{\mathrm{p}1}\\ d_{\mathrm{s}2}\\ d_{\mathrm{p}2}\end{bmatrix}=\begin{bmatrix}A_1-A_2\\ B_1-B_2\\ C_1-\mu C_2\\ D_1-\mu D_2\end{bmatrix}, \tag{8}$$

where $\mu=\mu_2/\mu_1$ is the ratio of the shear moduli of the half-planes, $C_i=b_i^2A_i\omega/V+(b_i^2-2)k_zB_i$, $D_i=k_zA_i+B_i\omega/V$. Eq. (8) can be readily solved to give the unknown constants $d_{\mathrm{s}i}$ and $d_{\mathrm{p}i}$. Thus, the solution of the problem given by Eqs. (1) and (2) can be considered to be known analytically in the frequency–wavenumber domain.

As one can see from Eq. (5), the displacement of each half-plane is the superposition of three terms:

$$\tilde{\tilde{\mathbf{u}}}_i = \tilde{\tilde{\mathbf{u}}}_{\mathrm{F}i} + \tilde{\tilde{\mathbf{u}}}_{\mathrm{s}i} + \tilde{\tilde{\mathbf{u}}}_{\mathrm{p}i}. \tag{9}$$

In Eq. (9), $\tilde{\tilde{\mathbf{u}}}_{\mathrm{F}i} = A_i \exp(\mathrm{i}\omega x/V)$ is the eigenfield of the load that is stationary in the reference system that moves with the load. The energy of this eigenfield changes as the load crosses the interface $x = 0$, which can be thought of as the reason for transition radiation. The terms $\tilde{\tilde{\mathbf{u}}}_{\mathrm{s}i} = d_{\mathrm{s}i}\mathbf{C}_{\mathrm{s}i} \exp(-\mathrm{i}R_{\mathrm{s}i}|x|)$ and $\tilde{\tilde{\mathbf{u}}}_{\mathrm{p}i} = d_{\mathrm{p}i}\mathbf{C}_{\mathrm{p}i} \exp(-\mathrm{i}R_{\mathrm{p}i}|x|)$ contain trains of waves that, though excited by the load, propagate independently of it. These are the propagating waves in the latter two terms that describe transition radiation.

The transition radiation field consists of two distinct parts, namely of the body waves and of the interface waves (the latter occurs only in a specific range of the continuum parameters). The body waves propagate from the interface towards infinities. The z-component of the phase velocity $c_i = \omega/k_z$ of these waves must satisfy the condition $c_i^2/c_{\mathrm{s}i,\mathrm{p}i}^2 > 1$. The interface waves propagate along the interface and decay exponentially with the distance from the interface. The phase velocity of these waves equals the velocity of Stoneley waves [6], which is smaller than the minimum shear wave speed in the continuum. Correspondingly, the continuum parameters $\mathbb{N}_{\mathrm{St}}$ that give rise to this part of transition radiation are the same as those required for existence of Stoneley waves (see Ref. [7]).

Both parts of transition radiation can be extracted from the following displacement field that is obtained by inverting the free-wave part of Eq. (9) into the time–space domain:

$$\mathbf{u}_i^{\mathrm{free}} = (2\pi)^{-2} \int_{-\infty}^{\infty}\int_{-\infty}^{\infty} \left(\tilde{\tilde{\mathbf{u}}}_{\mathrm{s}i} + \tilde{\tilde{\mathbf{u}}}_{\mathrm{p}i}\right) \exp(-\mathrm{i}(\omega t - k_z z))\,\mathrm{d}\omega\,\mathrm{d}k_z. \tag{10}$$

This expression is used in the following sections to derive the energy of transition radiation.

3. Transition radiation of body waves

To determine the energy of body waves that are excited during the load transition through the interface, it is convenient to use the so-called Hamilton's approach [8]. According to this approach, the radiation energy is calculated by integrating the energy density of the elastic field over space rather than integrating the energy flux through a surface over time. The Hamilton's method is based on the idea to consider the radiation field sufficiently long after the load has passed through the interface between the half-planes. Mathematically, the field is considered in the limit of $t \to \infty$. In this limit, the four wave fields that participate in the system dynamics, namely the eigenfield of the load, the shear wave field, the pressure wave field and the interface wave field (if generated), can be considered to separate in space owing to the different propagation speeds. Thus, the energies of each field can be computed separately and the energy of transition radiation transferred by the body waves E_i^r can be expressed as

$$E_i^r = E_{\mathrm{s}i}^r + E_{\mathrm{p}i}^r, \tag{11}$$

$$E_{\mathrm{s}i,\mathrm{p}i}^r = \int_{-\infty}^{\infty}\int_{-\infty}^{\infty} e_{\mathrm{s}i,\mathrm{p}i}^r(x,z,t)\,\mathrm{d}x\,\mathrm{d}z, \tag{12}$$

where $e_{\mathrm{s}i}^r(x,z,t)$ and $e_{\mathrm{p}i}^r(x,z,t)$ are the densities of radiation energy associated with the shear and pressure waves, respectively. Note that the limits of integration over x in Eq. (12) span from minus to plus infinity instead of covering the corresponding half-planes. The integration interval is extended for convenience of the mathematical elaborations to follow. The extension is justified by the fact that in the limit $t \to \infty$, the radiation pulses are so far from the interface that integration over the complete plane and that over the corresponding half-plane give exactly the same results. The superscript r in Eq. (11) specifies that not the complete elastic fields $\mathbf{u}_{\mathrm{s}i}$ and $\mathbf{u}_{\mathrm{p}i}$ are accounted for but only the propagating parts of these that are associated with radiation into the half-planes, e.g.

$$\mathbf{u}_{\mathrm{s}i}^r = (2\pi)^{-2} \int_{-\infty}^{\infty}\int_{-|\omega|/c_{\mathrm{s}i}}^{|\omega|/c_{\mathrm{s}i}} \tilde{\mathbf{u}}_{\mathrm{s}i}(\omega,k_z) \exp(-\mathrm{i}(\omega t - k_z z))\,\mathrm{d}k_z\,\mathrm{d}\omega. \tag{13}$$

The energy density $e(x,z,t)$ of the elastic continuum is the superposition of the kinetic energy density $\kappa(x,z,t)$ and the potential energy density $p(x,z,t)$. In terms of the continuum displacements, these densities read (see Ref. [9]):

$$\begin{aligned}\kappa_i &= \tfrac{1}{2}\rho_i(\partial_t u_i)^2 + \tfrac{1}{2}\rho_i(\partial_t w_i)^2,\\ p_i &= \tfrac{1}{2}\lambda_i(\partial_x u_i + \partial_z w_i)^2 + \tfrac{1}{2}\mu_i(\partial_z u_i + \partial_x w_i)^2 + \mu_i\big((\partial_x u_i)^2 + (\partial_z w_i)^2\big).\end{aligned} \tag{14}$$

To calculate the energy of transition radiation, the shear wave field and the pressure wave field defined by Eq. (10) should be separately substituted into Eq. (14) and then integrated in accordance with Eq. (12).

To evaluate the quadratic terms of which the energy density is composed, a method described in Ref. [1] is used. According to this method, the term $(\partial_t u_{si})^2$, for example, can be written as

$$\begin{aligned}(\partial_t u_{si})^2 &= (\partial_t u_{si})(\partial_t u_{si})^*,\\ \partial_t u_{si} &= (2\pi)^{-2}\int_{-\infty}^{\infty}\int_{-\infty}^{\infty}(-\mathrm{i}\omega)\tilde{\tilde{u}}_{si}(\omega,k_z)\exp\left(-\mathrm{i}(\omega t - k_z z)\right)\mathrm{d}\omega\,\mathrm{d}k_z,\\ (\partial_t u_{si})^* &= (2\pi)^{-2}\int_{-\infty}^{\infty}\int_{-\infty}^{\infty}(\mathrm{i}\bar{\omega})\tilde{\tilde{u}}^*_{si}(\bar{\omega},\bar{k}_z)\exp\big(\mathrm{i}\big(\bar{\omega}t - \bar{k}_z z\big)\big)\,\mathrm{d}\bar{\omega}\,\mathrm{d}\bar{k}_z,\end{aligned} \tag{15}$$

where the asterisk implies complex conjugation. Consequently, $(\partial_t u_{si})^2$ can be written as

$$(\partial_t u_{si})^2 = (2\pi)^{-4}\int_{-\infty}^{\infty}\int_{-\infty}^{\infty}\int_{-\infty}^{\infty}\int_{-\infty}^{\infty}\omega\bar{\omega}\tilde{\tilde{u}}_{si}(\omega,k_z)\tilde{\tilde{u}}^*_{si}(\bar{\omega},\bar{k}_z)\,\mathrm{e}^{\mathrm{i}t(\bar{\omega}-\omega)+\mathrm{i}z(k_z-\bar{k}_z)}\,\mathrm{d}\bar{k}_z\,\mathrm{d}k_z\,\mathrm{d}\bar{\omega}\,\mathrm{d}\omega. \tag{16}$$

To distinguish the propagating part of the displacement field, only those frequencies and wave-numbers should be accounted for in Eq. (16) that correspond to real values of R_{si}, i.e. $\omega^2 > c_{si}^2 k_z^2$. Therefore, the part $\big(\partial_t u^r_{si}\big)^2$ of Eq. (16) that corresponds to propagating waves into the half-planes can be written as

$$\big(\partial_t u^r_{si}\big)^2 = (2\pi)^{-4}\int_{-\infty}^{\infty}\int_{-\infty}^{\infty}\int_{-|\omega|/c_{si}}^{|\omega|/c_{si}}\int_{-|\bar{\omega}|/c_{si}}^{|\bar{\omega}|/c_{si}}\omega\bar{\omega}\tilde{\tilde{u}}_{si}(\omega,k_z)\tilde{\tilde{u}}^*_{si}(\bar{\omega},\bar{k}_z)\,\mathrm{e}^{\mathrm{i}t(\bar{\omega}-\omega)+\mathrm{i}z(k_z-\bar{k}_z)}\,\mathrm{d}\bar{k}_z\,\mathrm{d}k_z\,\mathrm{d}\bar{\omega}\,\mathrm{d}\omega. \tag{17}$$

Applying the above-described procedure to the complete energy density defined by Eq. (14), the energy densities of radiated shear and pressure wave fields can be written as

$$e^r_{\mathrm{s}i,\mathrm{p}i} = \frac{1}{(2\pi)^4}\int_{-\infty}^{\infty}\int_{-\infty}^{\infty}\int_{-|\omega|/c_{si,\mathrm{p}i}}^{|\omega|/c_{si,\mathrm{p}i}}\int_{-|\bar{\omega}|/c_{si,\mathrm{p}i}}^{|\bar{\omega}|/c_{si,\mathrm{p}i}}\beta_{si,\mathrm{p}i}\,d_{si,\mathrm{p}i}\bar{d}^*_{si,\mathrm{p}i}\,W_{si,\mathrm{p}i}\,\mathrm{e}^{\mathrm{i}t(\bar{\omega}-\omega)+\mathrm{i}z(k_z-\bar{k}_z)}\,\mathrm{d}\bar{k}_z\,\mathrm{d}k_z\,\mathrm{d}\bar{\omega}\,\mathrm{d}\omega, \tag{18}$$

where

$$W_{si,\mathrm{p}i} = \begin{cases}\mathrm{e}^{\mathrm{i}x\left(\bar{R}_{\mathrm{s}1,\mathrm{p}1}-R_{\mathrm{s}1,\mathrm{p}1}\right)}, & i=1,\\ \mathrm{e}^{\mathrm{i}x\left(R_{\mathrm{s}2,\mathrm{p}2}-\bar{R}_{\mathrm{s}2,\mathrm{p}2}\right)}, & i=2,\end{cases} \tag{19}$$

$$\beta_{\mathrm{s}i}(\omega,\bar{\omega},k_z,\bar{k}_z) = \frac{1}{2}\rho_i\omega\bar{\omega}\left(1+\frac{R_{si}\bar{R}_{\mathrm{s}i}}{k_z\bar{k}_z}\right)+\frac{1}{2}\mu_i k_z\bar{k}_z\left(1+4\frac{R_{si}\bar{R}_{\mathrm{s}i}}{k_z\bar{k}_z}-2\frac{\bar{R}^2_{si}}{\bar{k}_z^2}+\frac{R^2_{si}\bar{R}^2_{si}}{k_z^2\bar{k}_z^2}\right), \tag{20}$$

$$\begin{aligned}\beta_{\mathrm{p}i}(\omega,\bar{\omega},k_z,\bar{k}_z) = {}& \frac{1}{2}\rho_i\omega\bar{\omega}\left(1+\frac{k_z\bar{k}_z}{R_{\mathrm{p}i}\bar{R}_{\mathrm{p}i}}\right)+\frac{1}{2}\lambda_i R_{\mathrm{p}i}\bar{R}_{\mathrm{p}i}\left(1+2\frac{\bar{k}_z^2}{\bar{R}^2_{\mathrm{p}i}}+\frac{k_z^2\bar{k}_z^2}{R^2_{\mathrm{p}i}\bar{R}^2_{\mathrm{p}i}}\right)\\ &+\mu_i R_{\mathrm{p}i}\bar{R}_{\mathrm{p}i}\left(1+2\frac{k_z\bar{k}_z}{R_{\mathrm{p}i}\bar{R}_{\mathrm{p}i}}+\frac{k_z^2\bar{k}_z^2}{R^2_{\mathrm{p}i}\bar{R}^2_{\mathrm{p}i}}\right)\end{aligned} \tag{21}$$

and $\bar{R}_{si,\mathrm{p}i} = R_{si,\mathrm{p}i}(\bar{\omega},\bar{k}_z)$, $\bar{d}^*_{si,\mathrm{p}i} = d^*_{si,\mathrm{p}i}(\bar{\omega},\bar{k}_z)$, where $d_{si,\mathrm{p}i}$ are the solutions of Eq. (8).

The energy of transition radiation carried by the body waves is obtained by substituting Eq. (18) into Eq. (12). This substitution followed by integration over x and z results in:

$$E^r_{si,pi}=\frac{1}{(2\pi)^2}\int_{-\infty}^{\infty}\int_{-\infty}^{\infty}\int_{-|\omega|/c_{si,pi}}^{|\omega|/c_{si,pi}}\int_{-|\bar\omega|/c_{si,pi}}^{|\bar\omega|/c_{si,pi}}\beta_{si,pi}\,d_{si,pi}\bar d^*_{si,pi}\,e^{it(\bar\omega-\omega)}\delta(k_z-\bar k_z)\delta(\bar R_{si,pi}-R_{si,pi})\,d\bar k_z\,dk_z\,d\bar\omega\,d\omega, \quad (22)$$

where $\delta(\ldots)$ is the Dirac delta-function. To obtain Eq. (22), the following integral representation of the Dirac delta-function was used: $2\pi\delta(a)=\int_{-\infty}^{\infty}\exp(\pm iax)\,dx$.

Employing the following properties of the Dirac delta-function:

$$\int_{-\infty}^{\infty}f(\bar k_z)\delta(k_z-\bar k_z)\,d\bar k_z=f(k_z),\quad \int_{-\infty}^{\infty}f(\bar\omega)\delta(g(\bar\omega)-g(\omega))\,d\bar\omega=\left.\frac{f(\bar\omega)}{|dg/d\bar\omega|}\right|_{\bar\omega=\omega}. \quad (23)$$

Eq. (22) can be reduced to

$$\begin{aligned}
&E^r_{si,pi}=\frac{1}{2\pi^2}\int_0^{\infty}\int_{-\omega/c_{si,pi}}^{\omega/c_{si,pi}}\gamma_{si,pi}(\omega,k_z)\left|d_{si,pi}(\omega,k_z)\right|^2 dk_z\,d\omega,\\
&\gamma_{si}(\omega,k_z)=\frac{1}{2}\rho_i c_{si}^2\omega R_{si}\left(1+\frac{R_{si}^2}{k_z^2}\right)+\frac{1}{2}\mu_i c_{si}^2\frac{R_{si}k_z^2}{\omega}\left(1+2\frac{R_{si}^2}{k_z^2}+\frac{R_{si}^4}{k_z^4}\right)=\rho_i\frac{\omega^3R_{si}}{k_z^2},\\
&\gamma_{pi}(\omega,k_z)=\frac{1}{2}\rho_i c_{pi}^2\omega R_{pi}\left(1+\frac{k_z^2}{R_{pi}^2}\right)+\frac{1}{2}\rho_i c_{pi}^4\frac{R_{pi}^3}{\omega}\left(1+\frac{k_z^2}{R_{pi}^2}\right)^2=\rho_i\frac{\omega^3}{R_{pi}}.
\end{aligned} \quad (24)$$

Note that in Eq. (24) the radiation energy is time independent. This result is transparent from the physical viewpoint because in the limit of $t\to\infty$, the energy of the radiation fields is constant owing to the spatial separation of the wave fields and absence of damping.

Conventionally, radiation energy is quantified by the directivity diagram, which shows the energy distribution in space for a particular frequency. The directivity diagram can be obtained from Eq. (24) by introducing the polar coordinate system in the wavenumber domain: $k_x=k\cos\varphi$, $k_z=k\sin\varphi$, where k is the length of the wavenumber vector that is equal to $|\omega|/c_{pi}$ for the pressure waves and to $|\omega|/c_{si}$ for the shear waves. Substitution of $k_z=|\omega|/c_{si,pi}\sin\varphi$ into Eq. (24) gives the following expressions:

$$\begin{aligned}
&E^r_{s1,p1}=\int_0^{\infty}\omega^{-1}\int_{\pi/2}^{3\pi/2}Q_{s1,p1}(\varphi)\,d\varphi\,d\omega,\quad E^r_{s2,p2}=\int_0^{\infty}\omega^{-1}\int_{-\pi/2}^{\pi/2}Q_{s2,p2}(\varphi)\,d\varphi\,d\omega,\\
&Q_{si}(\varphi)=\frac{\rho_i\omega^4}{2\pi^2}\left|d_{si}(\omega,\varphi)\right|^2\cot^2(\varphi),\quad Q_{pi}(\varphi)=\frac{\rho_i\omega^4}{2\pi^2}\left|d_{pi}(\omega,\varphi)\right|^2.
\end{aligned} \quad (25)$$

Eq. (25) shows that the spectral angular energy densities of radiation $Q_{si,pi}(\varphi)/\omega$ are separable into the frequency-dependent part ω^{-1} and the angular density $Q_{si,pi}(\varphi)$. This separability is due to the non-dispersive character of the continuum (two half-planes) under consideration. Owing to ω^{-1} in the integrands, the radiation energies $E^r_{si,pi}$ are divergent, which is a direct consequence of the divergent eigenfield of a point load in the elastic continuum.

The angular density of radiation forward, $Q_{s2,p2}(\varphi)$, and backward, $Q_{s1,p1}(\varphi)$, are different and depend on the parameters of the half-planes and the load velocity. These dependencies are analyzed in Section 5, together with the part of transition radiation propagated in the form of interface waves. An expression for the latter is obtained in the next section.

4. Transition radiation of interface waves

Transition radiation can also propagate in the form of interface waves provided that the continuum parameters satisfy the condition of existence of Stoneley waves [7]. The energy of this radiation can be calculated by considering the energy flux $S^{(\mathbf{e}_z)}_{St}(x,z,t)$ of interface waves through the planes $z\to\pm\infty$.

According to Ref. [9], the two parts of this flux that are associated with the motion of the left half-plane, $S_{\mathrm{St1}}^{(\mathbf{e}_z)}$, and right half-plane, $S_{\mathrm{St2}}^{(\mathbf{e}_z)}$, can be expressed in terms of the continuum displacement as

$$S_{\mathrm{St}i}^{(\mathbf{e}_z)} = -\big((\lambda_i + 2\mu_i)(\partial_z w_{\mathrm{St}i})(\partial_t w_{\mathrm{St}i}) + \lambda_i(\partial_x u_{\mathrm{St}i})(\partial_t w_{\mathrm{St}i}) + \mu_i(\partial_z u_{\mathrm{St}i} + \partial_x w_{\mathrm{St}i})\partial_t u_{\mathrm{St}i}\big), \tag{26}$$

where the vector-displacements $\mathbf{u}_{\mathrm{St}i}(x,z,t)$ describe the contribution of Stoneley waves to the elastic field given by Eq. (10). This contribution can be extracted from Eq. (10) by evaluating the integral over ω with the help of the contour integration method and the residue theorem [10].

The integral $\tilde{\mathbf{u}}_i^{\mathrm{free}}$ over ω in Eq. (10) can be distinguished by rewriting this equation as

$$\mathbf{u}_i^{\mathrm{free}} = (2\pi)^{-1}\int_{-\infty}^{\infty} \tilde{\mathbf{u}}_i^{\mathrm{free}} \exp(\mathrm{i}k_z z)\,\mathrm{d}k_z, \tag{27}$$

where

$$\tilde{\mathbf{u}}_i^{\mathrm{free}} = (2\pi)^{-1}\int_{-\infty}^{\infty} \big(\tilde{\mathbf{u}}_{\mathrm{s}i} + \tilde{\mathbf{u}}_{\mathrm{p}i}\big) \exp(-\mathrm{i}\omega t)\,\mathrm{d}\omega = \int_{-\infty}^{\infty} \mathbf{f}(\omega)\,\mathrm{d}\omega. \tag{28}$$

In accordance with the contour integration method, the latter integral can be evaluated by considering ω as a complex value and closing the original integration path in the complex ω-plane. It is convenient to close the integration contour by a semicircle located in the lower half-plane of the complex ω-plane as shown in Fig. 2. In this case, owing to the fact that positive time moments are considered (interface waves will reach the planes $z \to \pm\infty$ when $t \to +\infty$), the integral over this semicircle vanishes as its radius tends to infinity. Therefore, the integral in Eq. (28) can be represented as

$$\int_{-\infty}^{\infty} \mathbf{f}(\omega)\,\mathrm{d}\omega = -2\pi\mathrm{i} \operatorname*{Res}_{\substack{\omega=\omega_{\mathrm{poles}},\\ \mathrm{Im}(\omega_{\mathrm{poles}})<0}} (\mathbf{f}(\omega)) + \int_{\substack{\text{branch points}\\ \text{branch cuts}}} \mathbf{f}(\omega)\,\mathrm{d}\omega. \tag{29}$$

The first term on the right-hand side in Eq. (29) is the contribution of the poles located inside the chosen contour, whereas the second term comprises the integrals around the branch points and over branch cuts that would ensure that $\mathbf{f}(\omega)$ is a single-valued function in the ω-plane.

Transition radiation of interface waves occurs if $\mathbf{f}(\omega)$ has poles $\pm\omega_{\mathrm{St}}$ on real ω-axis. These poles can be found from the well-known Stoneley wave equation [6], which can also be obtained by equating the determinant of the 4×4 matrix in Eq. (8) to zero.

The contribution of the 'Stoneley' poles $\omega = \pm\omega_{\mathrm{St}}$ describes propagating interface waves generated during the load transition through the interface.

In Eq. (29) it is implicitly assumed that all poles have a non-zero imaginary part. This is correct provided that an infinitely small dissipation is taken into account that would shift the poles from the real axis. This dissipation must be accounted for in the Fourier analysis to avoid physically unrealistic waves propagating from infinity [8]. One may account for small dissipation by replacing the Young's modulus by the differential operator $E(1+\varepsilon\partial_t)$. This replacement would result in complex wave speeds in the frequency–wavenumber

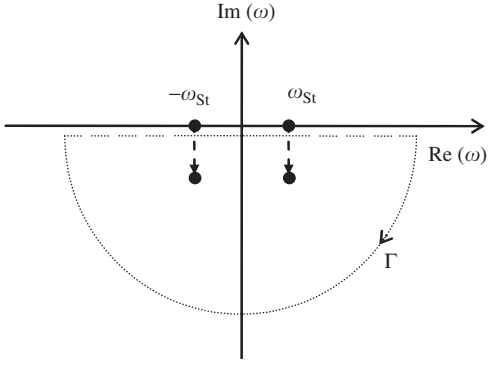

Fig. 2. Integration contour and position of the poles as used in calculation of transition radiation of the interface waves.

domain and would correspond to the following shift of the 'Stoneley' poles: $\pm\omega_{\mathrm{St}} \to \pm\omega_{\mathrm{St}} - \mathrm{i}\delta k_z^2\varepsilon$, where $\delta > 0$ is a real constant dependent on the continuum parameters. Thus, both 'Stoneley' poles shift to the lower half-plane independently of the sign of k_z, as shown in Fig. 2. Consequently, both these poles contribute to the elastic field associated with propagating interface waves.

According to the above-given explanation, the contribution $\tilde{\mathbf{u}}_{\mathrm{St}i}$ of the 'Stoneley' poles to $\tilde{\mathbf{u}}_i^{\mathrm{free}}$ in Eq. (28) is given as

$$\tilde{\mathbf{u}}_{\mathrm{St}i} = -\mathrm{i} \operatorname*{Res}_{\omega=\pm\omega_{\mathrm{St}}} \left(\left(\tilde{\tilde{\mathbf{u}}}_{\mathrm{s}i} + \tilde{\tilde{\mathbf{u}}}_{\mathrm{p}i} \right) \exp\left(-\mathrm{i}\omega t\right) \right). \tag{30}$$

Substituting $\tilde{\tilde{\mathbf{u}}}_{\mathrm{s}i} = d_{\mathrm{s}i}\mathbf{C}_{\mathrm{s}i} \exp\left(-\mathrm{i}R_{\mathrm{s}i}|x|\right)$ and $\tilde{\tilde{\mathbf{u}}}_{\mathrm{p}i} = d_{\mathrm{p}i}\mathbf{C}_{\mathrm{p}i} \exp\left(-\mathrm{i}R_{\mathrm{p}i}|x|\right)$, one can rewrite this equation as

$$\tilde{\mathbf{u}}_{\mathrm{St}i} = -\mathrm{i} \sum_{\mathrm{wave=s,p}} \operatorname*{Res}_{\omega=\pm\omega_{\mathrm{St}}} \left(d_{\mathrm{wave}\,i}\mathbf{C}_{\mathrm{wave}\,i} \exp\left(-\mathrm{i}R_{\mathrm{wave}\,i}|x|\right) \exp\left(-\mathrm{i}\omega t\right) \right), \tag{31}$$

where the summation sign implies the superposition of the shear wave- and pressure wave-related quantities.

Introduction of a notation $d_{si,\mathrm{p}i}(\omega, k_z) = f_{si,\mathrm{p}i}(\omega, k_z)/g(\omega, k_z)$, which underlines that all $d_{si,\mathrm{p}i}$ have the same denominator, allows to evaluate the residues in Eq. (31) and to write this equation as

$$\tilde{\mathbf{u}}_{\mathrm{St}i} = \frac{-\mathrm{i}}{\partial_\omega g\big|_{\omega=\omega_{\mathrm{St}}}} \sum_{\mathrm{wave=s,p}} \mathbf{C}_{\mathrm{wave}\,i} \exp\left(-\mathrm{i}\,R_{\mathrm{wave}\,i}|x|\right)\big|_{\omega=\omega_{\mathrm{St}}} \left(f_{\mathrm{wave}\,i} \exp\left(-\mathrm{i}\omega t\right)\big|_{\omega=\omega_{\mathrm{St}}} - f_{\mathrm{wave}\,i} \exp(-\mathrm{i}\,\omega t)\big|_{\omega=-\omega_{\mathrm{St}}} \right). \tag{32}$$

In obtaining Eq. (32), it was used that $\partial_\omega g$ is an odd function of ω, whereas $\mathbf{C}_{si,\mathrm{p}i}$ is an even function of ω.

Evaluating Eq. (8) with the help of symbolic software, the following representation can be shown to be valid:

$$\pm \frac{f_{si,\mathrm{p}i}(\omega, k_z)}{\partial_\omega g(\omega, k_z)}\bigg|_{\omega=\pm\omega_{\mathrm{St}}} = \frac{1}{k_z} \frac{s^{\pm}_{si,\mathrm{p}i}}{h(c_{\mathrm{St}})}, \quad s^{\pm}_{si,\mathrm{p}i} = p_{si,\mathrm{p}i}(c_{\mathrm{St}}) \pm \mathrm{i}\frac{k_z}{|k_z|} q_{si,\mathrm{p}i}(c_{\mathrm{St}}), \tag{33}$$

where $c_{\mathrm{St}} = \omega_{\mathrm{St}}/k_z$ is the Stoneley wave speed. The real functions $h(c_{\mathrm{St}})$, $p_{si,\mathrm{p}i}(c_{\mathrm{St}})$ and $q_{si,\mathrm{p}i}(c_{\mathrm{St}})$ can be identified symbolically by evaluating Eq. (8).

Substituting Eq. (32) into Eq. (27) and using Eq. (33), the following expression is obtained for the elastic field associated with transition radiation of interface (Stoneley) waves:

$$\mathbf{u}_{\mathrm{St}i} = \frac{-\mathrm{i}}{2\pi h(c_{\mathrm{St}})} \sum_{\mathrm{wave=s,p}} \int_{-\infty}^{\infty} \frac{\mathbf{C}_{\mathrm{wave}\,i}(\omega_{\mathrm{St}}, k_z)}{k_z} \mathrm{e}^{\mathrm{i}k_z z - |k_z x|\alpha_{\mathrm{wave}\,i}} \left(s^{+}_{\mathrm{wave}\,i} \mathrm{e}^{-\mathrm{i}k_z c_{\mathrm{St}} t} + s^{-}_{\mathrm{wave}\,i} \mathrm{e}^{\mathrm{i}k_z c_{\mathrm{St}} t} \right) \mathrm{d}k_z, \tag{34}$$

where $\alpha_{si,\mathrm{p}i} = \sqrt{1 - c_{\mathrm{St}}^2/c_{si,\mathrm{p}i}^2}$ (the Stoneley wave speed is always smaller than the body wave speeds). Obviously, Eq. (34) is the superposition of the Stoneley wave trains propagating downwards ($\mathbf{u}^{+}_{\mathrm{St}i}$, proportional to $s^{+}_{si,\mathrm{p}i}$) and upwards ($\mathbf{u}^{-}_{\mathrm{St}i}$, proportional to $s^{-}_{si,\mathrm{p}i}$). One can show that these wave trains carry the same energy. Therefore, in the following, only radiation downwards carried by the displacement field $\mathbf{u}^{+}_{\mathrm{St}i}$ is evaluated. According to Eq. (34), this field is given as

$$\mathbf{u}^{+}_{\mathrm{St}i} = \frac{-\mathrm{i}}{2\pi h(c_{\mathrm{St}})} \sum_{\mathrm{wave=s,p}} \int_{-\infty}^{\infty} \frac{\mathbf{C}_{\mathrm{wave}\,i}(\omega_{\mathrm{St}}, k_z)}{k_z} s^{+}_{\mathrm{wave}\,i}(\omega_{\mathrm{St}}, k_z) \exp\left(\mathrm{i}k_z(z - c_{\mathrm{St}}t) - |k_z x|\alpha_{\mathrm{wave}\,i}\right) \mathrm{d}k_z. \tag{35}$$

The energy E^{+}_{St} of the elastic field $\mathbf{u}^{+}_{\mathrm{St}i}$ can be calculated by integrating the energy flux of this field through the plane $z \to \pm\infty$. The integral to be evaluated reads:

$$E^{+}_{\mathrm{St}} = \int_{-\infty}^{\infty} \left(\int_{-\infty}^{0} S^{(\mathbf{e}_z)}_{\mathrm{St}1}\Big|_{z\to+\infty} \mathrm{d}x + \int_{0}^{\infty} S^{(\mathbf{e}_z)}_{\mathrm{St}2}\Big|_{z\to+\infty} \mathrm{d}x \right) \mathrm{d}t, \tag{36}$$

where $S^{(\mathbf{e}_z)}_{\mathrm{St}i}$ are given by Eq. (26) with the vector-displacement defined by Eq. (35).

The procedure of evaluation of Eq. (36) is similar to that described in Section 3. First, Eq. (35) is substituted into the expression for the flux, Eq. (26). This gives a double integral over k_z and $\bar{k}_z$. The latter integral is substituted in Eq. (36) to give two quadruple integrals. As the next step, integration is accomplished in each of

these two integrals over time using the following integral representation of the Dirac delta-function: $2\pi\delta(k_z-\bar{k}_z)=\int_{-\infty}^{\infty}\exp(\pm \mathrm{i}t(k_z-\bar{k}_z))\,\mathrm{d}t$. Then, with the help of the obtained delta-function, integration over $\bar{k}_z$ is accomplished to give two double integrals over k_z and x. Note that these integrals do not depend on z. Finally, integration over x can be easily accomplished as the integrands depend on x exponentially (see Eq. (35)). The resulting expression can be written as

$$E^{+}_{\mathrm{St}}=\left(P^{+}_{\mathrm{St1}}+P^{+}_{\mathrm{St2}}\right)\int_0^{\infty}k_z^{-1}\,\mathrm{d}k_z, \tag{37}$$

where

$$P^{+}_{\mathrm{St}i}=\frac{\mu_i}{\pi h^2(c_{\mathrm{St}})}\left(\frac{1+3\alpha_{si}^2}{2\alpha_{si}}\left|s^{+}_{si}\right|^2+\frac{b_i^2-\alpha_{\mathrm{p}i}^2\left(b_i^2-4\right)}{2\alpha_{\mathrm{p}i}^3}\left|s^{+}_{\mathrm{p}i}\right|^2+\frac{2\left(b_i^2\alpha_{si}+\alpha_{\mathrm{p}i}\right)}{\alpha_{\mathrm{p}i}\left(\alpha_{si}+\alpha_{\mathrm{p}i}\right)}\,\mathrm{Re}\left(s^{+}_{si}\left(s^{+}_{\mathrm{p}i}\right)^{*}\right)\right.$$
$$\left.+\frac{\alpha_i\mathrm{Re}\left\{s^{+}_{si}\left(s^{+}_{\mathrm{p}i}\right)^{*}+\alpha_{si}^2s^{+}_{\mathrm{p}i}\left(s^{+}_{si}\right)^{*}\right\}-\left(b_i^2-2\right)\alpha_{si}\,\mathrm{Re}\left\{\alpha_{\mathrm{p}i}^2s^{+}_{si}\left(s^{+}_{\mathrm{p}i}\right)^{*}+s^{+}_{\mathrm{p}i}\left(s^{+}_{si}\right)^{*}\right\}}{\alpha_{\mathrm{p}i}\left(\alpha_{si}+\alpha_{\mathrm{p}i}\right)}\right),$$
$$s^{+}_{si,\mathrm{p}i}=p_{si,\mathrm{p}i}(c_{\mathrm{St}})+\mathrm{i}q_{si,\mathrm{p}i}(c_{\mathrm{St}}),\quad \alpha_{si,\mathrm{p}i}=\sqrt{1-c_{\mathrm{St}}^2\big/c_{si,\mathrm{p}i}^2},\quad b_i=c_{\mathrm{p}i}/c_{si}. \tag{38}$$

One can see from Eq. (37) that dependence of the energy of the radiated interface waves on the system parameters is fully characterized by $P^{+}_{\mathrm{St}i}$. The integral in this equation just shows that E^{+}_{St} is divergent as well as the energy carried by the pressure and shear waves.

In the next section the energy of transition radiation carried by both the body waves and the interface waves is analyzed for a number of specific parameters of the system.

5. Parametric analysis of radiation energy

The energy of transition radiation is analyzed in this section as a function of two dimensionless parameters, namely $V/\min\{c_{\mathrm{s}1},c_{\mathrm{s}2}\}$ and $c_{\mathrm{s}2}/c_{\mathrm{s}1}=\sqrt{\mu_2\rho_1/\mu_1\rho_2}$. The first parameter is the ratio of the load speed and the smallest shear wave speed. It characterizes how fast the load moves with respect to the body waves. The second parameter is the ratio of the shear wave speeds in the half-planes. It characterizes parameters of the half-planes.

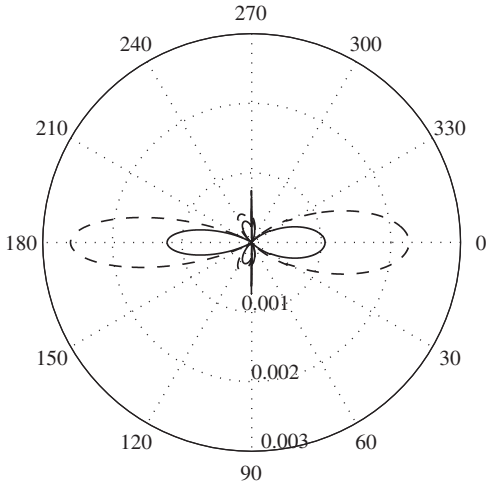

Fig. 3. The angular energy density Q_s (J m^{-1}) of the shear waves: (——) $V=0.6\,c_{\mathrm{s}1}$ and (– – –) $V=0.7\,c_{\mathrm{s}1}$.

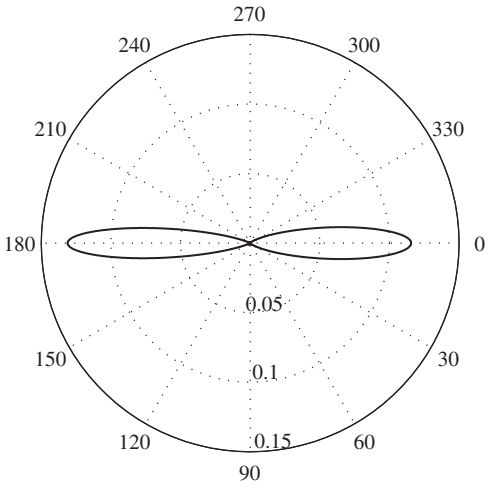

Fig. 4. The angular energy density Q_s ($\mathrm{J\,m^{-1}}$) of the shear waves for $V = 0.95\,c_{s1}$.

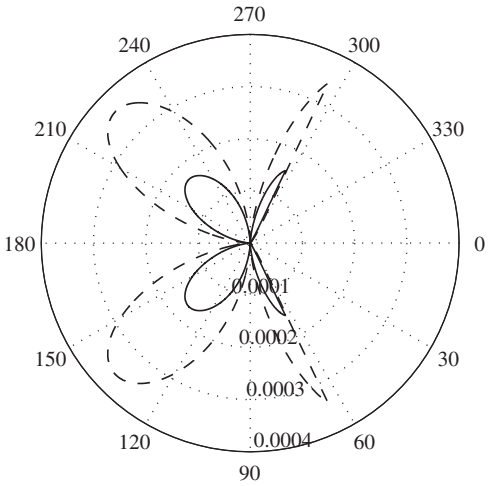

Fig. 5. The angular energy density Q_p ($\mathrm{J\,m^{-1}}$) of the pressure waves: (——) $V = 0.6\,c_{s1}$ and (– – –) $V = 0.7\,c_{s1}$.

Figs. 3–6 show the directivity diagrams $Q_{si,pi}(\varphi)$ for a number of velocities of the load. These diagrams are plotted in correspondence with Eq. (25) and using parameters given in Table 1. The load magnitude is chosen as $F_z = 1 \times 10^4\,\mathrm{N\,m^{-1}}$ and unaltered throughout this section.

Parameters in Table 1 correspond to loosely packed sand ($i = 1$) and slightly more densely packed sand ($i = 2$) and are chosen such that Stoneley waves may exist.

In Figs. 3 and 4 the directivity diagram of radiated shear waves is depicted for three velocities of the load, namely $V = 0.6c_{s1}$, $V = 0.7c_{s1}$ and $V = 0.95c_{s1}$. These figures show that radiation backward and forward is different. This is natural given different parameters of the half-planes and a non-zero load speed. One can also see that though the largest amount of energy is radiated along the load path, there is another direction, in which the radiation energy has its maximum (clearly visible in Fig. 3 for radiation backward). This maximum is not anomalous and occurs because of interaction of shear and pressure waves near the interface. Another feature of the directivity diagram is that it is symmetric with respect to the load path. This has to be so because the radiation energy is proportional to F_z^2 and, therefore, must possess this symmetry to be invariant with respect to the sign of F_z. Finally, Figs. 3 and 4 show that the closer the load speed to the minimum shear speed in the system the larger the radiation energy. This is a well-known feature of transition radiation [1,5].

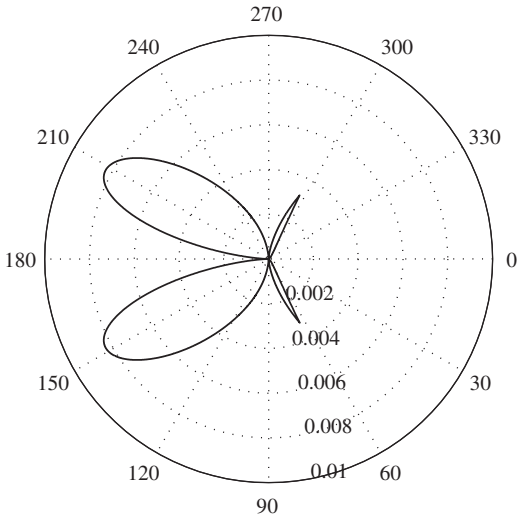

Fig. 6. The angular energy density Q_p (J m^{-1}) of the pressure waves for $V = 0.95\,c_{s1}$.

Table 1
Parameter values for Figs. 3–9

	E_i (N m^{-2})	ρ_i (kg m^{-3})	ν_i	μ_i (N m^{-2})	c_{si} (m s^{-1})	c_{pi} (m s^{-1})
$i=1$	5×10^7	1700	0.35	1.852×10^7	104.370	217.3
$i=2$	5.55×10^7	1960	0.30	2.135×10^7	104.374	195.3

Figs. 5 and 6 show the directivity diagram of radiated pressure waves for the same three velocities of the load as above. One can see that the energy of pressure waves is much smaller than that of the shear waves (compare Fig. 5 to Fig. 3, for example). This can be attributed to the direction of the load action, which is tangential to the interface. Further, in contrast to energy distribution in the pulse of shear waves, the maximum of radiation is directed not along the load path but sideways. The angle corresponding to this maximum depends on the parameters of the half-planes. The symmetry of the directivity diagram with respect to the loading path can be explained using the same reasoning as for shear waves.

In Fig. 7 the energy of the interface waves is compared to that of the body waves. For the sake of clarity only energy of shear waves radiated into the left half-plane is depicted (these waves are most powerful for the chosen set of parameters: $c_{s1} = \min\{c_{s1}, c_{s2}\}$). The energy of the interface waves is characterized by $P_{St} = P^+_{St1} + P^+_{St2}$, in accordance with Eq. (37). To enable comparison, the energy of the shear waves is characterized by the following integral of the angular density (see Eq. (25)):

$$P_{s1} = \int_{\pi/2}^{3\pi/2} Q_{s1}(\varphi)\,\mathrm{d}\varphi. \tag{39}$$

Both P_{St} and P_{s1} are made dimensionless by multiplying by μ_1/F_z^2 and depicted as functions of $V/\min\{c_{s1}, c_{s2}\}$ using parameters given in Table 1. Fig. 7 shows that for relatively low velocities of the load almost all energy of transition radiation is carried by the Stoneley waves. However, the closer the load velocity to the velocity of body waves, the greater the energy of the body waves. In the limit of $V \to c_{s1}$, transition radiation of the body waves becomes very powerful. The energy of the Stoneley waves stays bounded also for $V \to c_{St}$, because the load is moving along a path that is perpendicular to the direction of propagation. As a consequence resonance cannot occur.

To investigate dependence of transition radiation on the direction of the load motion, it is illustrative to interchange parameters of the half-planes. The result is shown in Figs. 8 and 9 that are plotted using

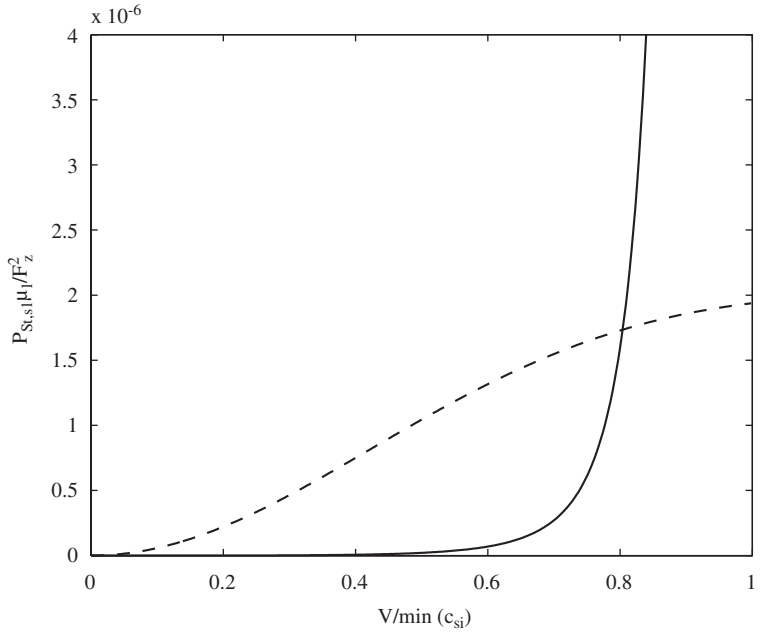

Fig. 7. Normalized energies of the interface and shear waves versus normalized load velocity: (——) $P_{s1}\mu_1/F_z^2$ and (– – –) $P_{St}\mu_1/F_z^2$.

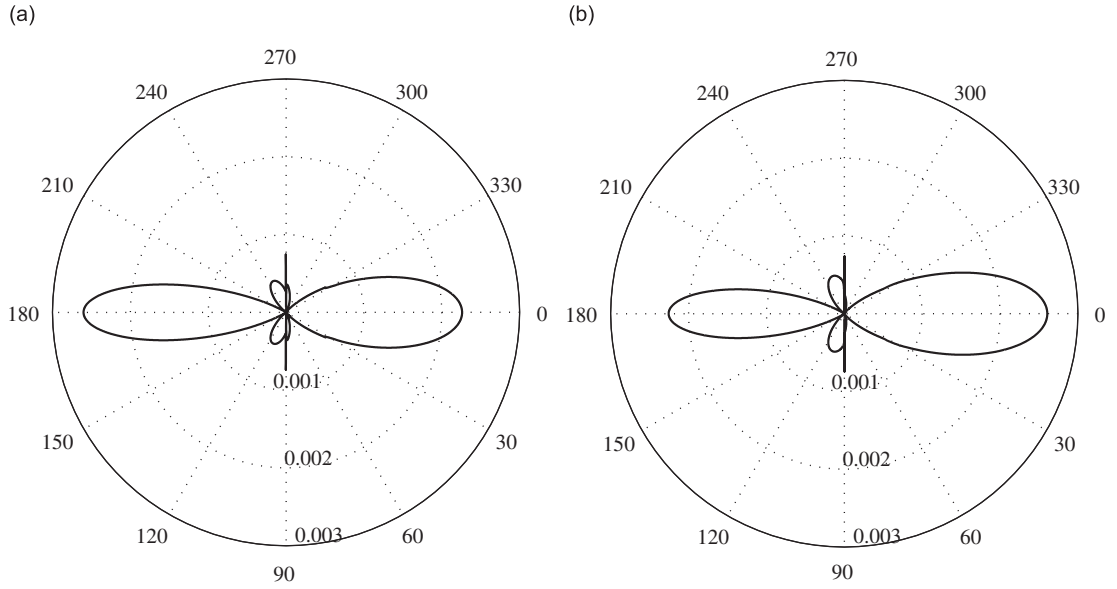

Fig. 8. The angular energy density Q_s ($J\,m^{-1}$) of shear waves for $V = 0.7\min\{c_{s1}, c_{s2}\}$: (a) original parameters of the half-planes and (b) interchanged parameters.

parameters specified in Table 1. In Fig. 8(a), the directivity diagram of the shear waves is depicted for the original parameters of the half-planes and $V = 0.7\min\{c_{s1}, c_{s2}\}$. In Fig. 8(b), this diagram is shown for the interchanged parameters (the right half-plane is given parameters of the left half-plane and vice versa). One can see that though the diagrams in Fig. 8 differ, the difference is marginal. Note that if the difference in parameters of the half-planes would be more pronounced than that given by Table 1, interchanging the half-planes would correspond to a larger difference in the directivity diagram.

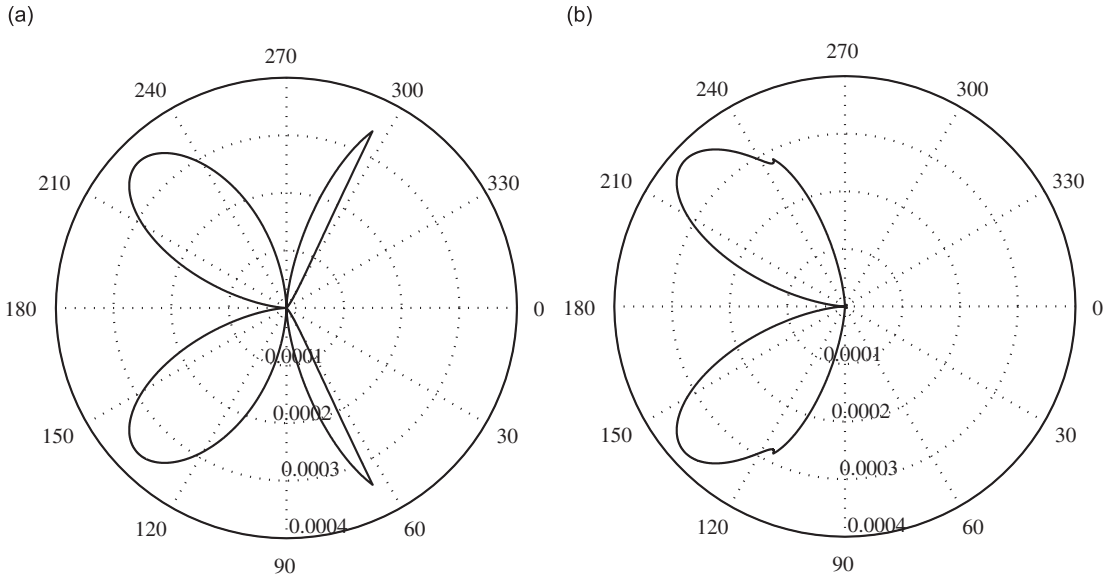

Fig. 9. The angular energy density Q_p (J m^{-1}) of pressure waves for $V = 0.7 \min\{c_{s1}, c_{s2}\}$: (a) original parameters of the half-planes and (b) interchanged parameters.

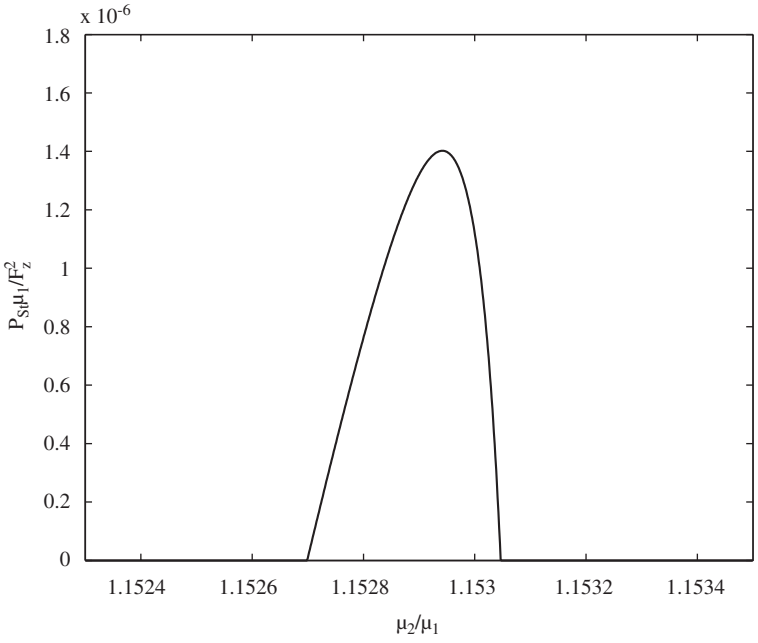

Fig. 10. Normalized energy of the interface waves versus the stiffness ratio of the half-planes.

The pressure waves are much more susceptible to the interchange of the half-planes. This can be seen in Fig. 9, which presents the directivity diagram of the radiated pressure waves (this figure is plotted in the same manner and using the same parameters as Fig. 8). Indeed, Figs. 9(a) and (b) differ dramatically, especially regarding the radiation forward that nearly disappears after the interchange of parameters.

The interface wave radiation is not influenced by the interchange of the parameters of the half-planes. It depends strongly, however, on the stiffness ratio μ_2/μ_1 and the mass density ratio ρ_2/ρ_1 of the half-planes. To show this dependence, Figs. 10 and 11 are plotted assuming the load velocity to be equal to $V = 50\,\mathrm{m\,s^{-1}}$.

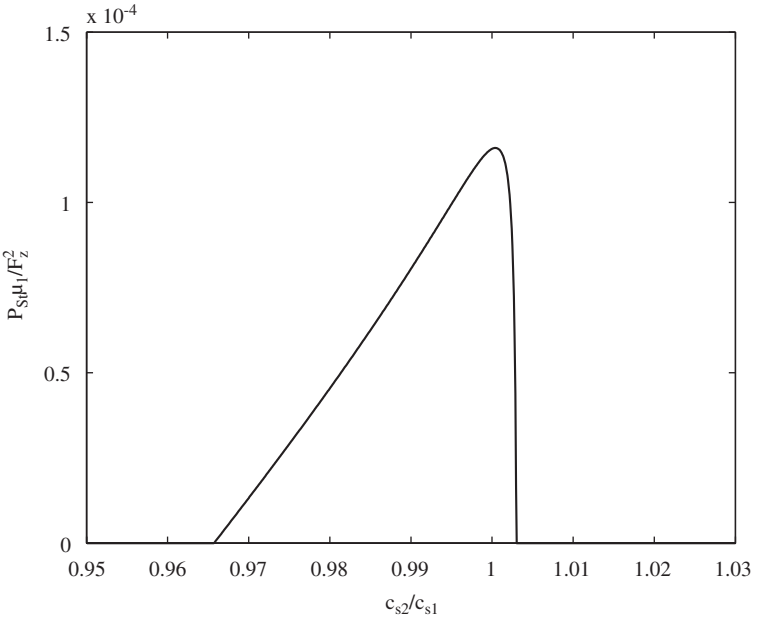

Fig. 11. Normalized energy of the interface waves versus the ratio of shear wave velocities in the half-planes.

Table 2
Parameters of the right half-plane for Figs. 10 and 11

	E_2 (N m^{-2})	ρ_2 (kg m^{-3})	ν_2	μ_2 (N m^{-2})	c_{s2} (m s^{-1})	c_{p2} (m s^{-1})
Fig. 10	Co-vary	1960	0.30	Vary	Co-vary	Co-vary
Fig. 11	8×10^7	Vary	0.30	3.077×10^7	Co-vary	Co-vary

Table 3
Parameters of the right half-plane for Figs. 12 and 13

E_2 (N m^{-2})	ρ_2 (kg m^{-3})	ν_2	μ_2 (N m^{-2})	c_{s2} (m s^{-1})	c_{p2} (m s^{-1})
Vary	1960	0.30	Co-vary	Co-vary	Co-vary

Parameters of the left half-plane are taken from Table 1 (for $i = 1$), whereas parameters of the right half-plane are varied as specified in Table 2.

The energy of the interface waves is characterized by the dimensionless ratio $P_{St}\mu_1/F_z^2 = (P_{St1}^+ + P_{St2}^+)\mu_1/F_z^2$, where P_{Sti}^+ are defined by Eq. (37). Fig. 10 presents dependence of the normalized P_{St} on the stiffness ratio μ_2/μ_1, whereas Fig. 11 shows P_{St} versus c_{s2}/c_{s1} (only ρ_2/ρ_1 is varied to change c_{s2}/c_{s1}).

Figs. 10 and 11 show that transition radiation of the interface waves exists in a relatively narrow domain of parameters of the half-planes. As mentioned earlier, this domain is distinguished by existence of Stoneley waves in the system. The energy of transition radiation reaches its maximum somewhere within this domain of parameters.

As the last step of the parametric analysis, dependence is studied of the radiation energy transferred by the body waves on the contrast of parameters of the half-planes. This contrast is characterized by the ratio of the shear wave speeds c_{s2}/c_{s1}. Parameters of the left half-plane are taken from Table 1 (for $i = 1$) whereas parameters of the right half-plane are varied as specified in Table 3.

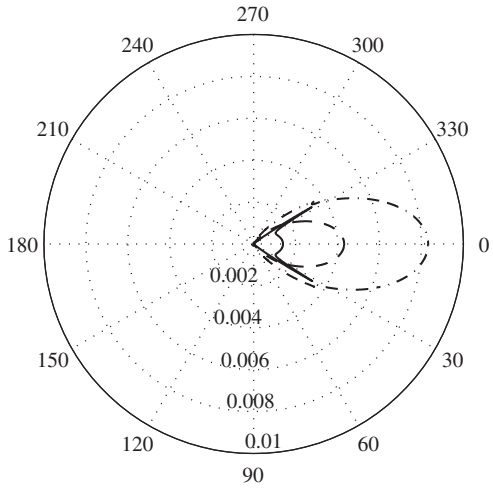

Fig. 12. The angular energy density Q_{s2} ($\mathrm{J\,m^{-1}}$) of shear waves radiated forward for increasing c_{s2}/c_{s1}: (– –) $c_{s2}/c_{s1} = 1.10$; (–·–·–·), c_{s2}/c_{s1}; (——) $c_{s2}/c_{s1} = 11.0$.

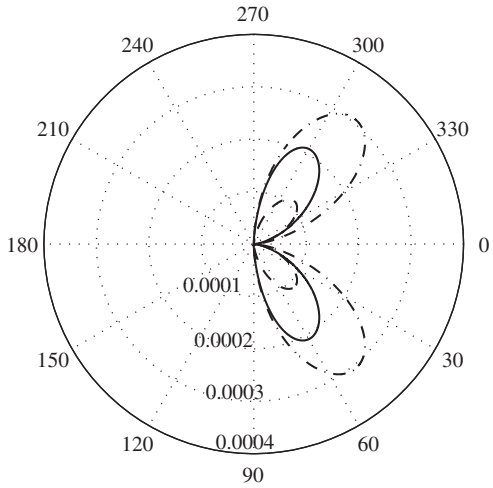

Fig. 13. The angular energy density Q_{p2} ($\mathrm{J\,m^{-1}}$) of pressure waves radiated forward for increasing c_{s2}/c_{s1}: (– – –) $c_{s2}/c_{s1} = 1.10$; (–·–·–) $c_{s2}/c_{s1} = 1.20$; (——) $c_{s2}/c_{s1} = 11.0$.

Figs. 12 and 13 show directivity diagrams of the shear waves and pressure waves, respectively, for three ratios of c_{s2}/c_{s1}. Both figures have been plotted with $V = 50\,\mathrm{m\,s^{-1}}$.

One can see from Figs. 12 and 13 that the radiation energy depends strongly on the contrast of parameters of the half-spaces. This contrast influences both the amount of energy radiated into a certain angle and the shape of the directivity diagram (Fig. 12). The energy distribution between the shear and pressure waves is also affected. Finally, it is important to note that dependence of the energy densities $Q_{s,p}$ on the contrast of parameters is not monotonic. Increase of the contrast does not necessarily lead to increase of the radiation energy.

6. Conclusions and discussion

Transition radiation of elastic waves that occurs as a load crosses the interface of two elastic half-planes has been investigated in this paper. It has been shown that the body waves are emitted by the load irrespective of its velocity and parameters of the half-planes. These waves are not radiated only if the load is not moving or

parameters of the half-planes do not differ. In addition to the body waves, interface waves can be radiated. Radiation of these waves occurs if parameters of the half-planes allow existence of Stoneley waves. If Stoneley waves may exist, transition radiation of interface waves occurs at any non-zero speed of the load. According to the authors' knowledge, transition radiation of interface waves has never been described in the past.

The study presented in this paper has shown that transition radiation in elastic continua has a number of specific features that are not present in transition radiation of electromagnetic and acoustic waves. These features stem from the fact that three types of waves may exist in an elastic continuum with interfaces, namely the pressure, shear and interface waves. These waves interfere in the process of formation of transition radiation. As a result of this interference, the energy and directivity of radiation transferred by these waves can depend on parameters of the continuum in a peculiar manner. In electrodynamics and acoustics, only one type of waves is normally radiated and the characteristics of these waves are much less peculiar than in elastodynamics. Thus, in the opinion of the authors of this paper, significant contribution can be made to the general theory of transitional radiation by studying it in elastic continua.

This paper has not been aimed at obtaining practically applicable results. On the contrary, the most simplistic model has been chosen to demonstrate as clearly as possible the main features of transition radiation in elastic continua. As a next step, more practically relevant models have to be investigated. For example, radiation can be studied from a load that moves over the surface of an inhomogeneous half-space (a superstructure between the load the half-space can be added as well). The half-space can be composed of two homogeneous quarter-spaces, have layers with interfaces that are not parallel to the surface or simply have some objects on the surface. In all these cases transition radiation would occur. The results of the above studies would be interesting for railway engineering because it would help predict generation of ground vibration by a train that moves over inhomogeneous subsoil and in a built environment.

Acknowledgement

The first author is grateful to the supervisors of his Ph.D. project, Dr. G.G. Drijkoningen and Prof. C.P.A. Wapenaar of the Applied Geophysics and Petrophysics section, for giving the opportunity to write this paper about his M.Sc. project.

References

[1] V.L. Ginzburg, V.N. Tsytovich, *Transition Radiation and Transition Scattering*, Hilger, Bristol, 1990.
[2] V.L. Ginzburg, I.M. Frank, Radiation arising from a uniformly moving electron as the electron crosses the boundary between two media, *Journal of Experimental and Theoretical Physics* 16 (1946) 15–30.
[3] V.P. Dokuchaev, On the theory of radiation of acoustic waves by small bodies that move in gaseous media, *Journal of Experimental and Theoretical Physics* 43 (1962) 595–604.
[4] A.I. Vesnitskii, A.V. Metrikine, Transition radiation in one-dimensional elastic systems, *Journal of Applied Mechanics and Technical Physics* 33 (1992) 202–207.
[5] A.I. Vesnitskii, A.V. Metrikine, Transition radiation in mechanics, *Physics-Uspekhi* 39 (10) (1996) 983–1007.
[6] R. Stoneley, Elastic waves at the surface of separation of two solids, *Proceedings of the Royal Society A* 106 (1924) 416–428.
[7] J.G. Scholte, The range of existence of Rayleigh and Stoneley waves, *Monthly Notices of Royal Astronomical Society: Geophysical Supplement* 5 (1947) 120–126.
[8] V.L. Ginzburg, *Theoretical Physics and Astrophysics*, Pergamon Press, Oxford, 1979.
[9] J.D. Achenbach, *Wave Propagation in Elastic Solids*, North-Holland Publishing Company, Amsterdam, 1973.
[10] B.A. Fuchs, B.V. Shabat, J. Berry, *Functions of a Complex Variable and some of their Applications*, Pergamon Press, Oxford, 1964.